Dental Materials Journal 2018; 37(4): 575–581

Surface modification of porous alpha-tricalcium phosphate granules with heparin enhanced their early osteogenic capability in a rat calvarial defect model

Yoshihiro TAKEDA[1], Yoshitomo HONDA[2], Sachiro KAKINOKI[3], Tetsuji YAMAOKA[3] and Shunsuke BABA[1]

[1] *Department of Oral Implantology, Osaka Dental University, 8-1, Kuzuhahanazonocho, Hirakata, Osaka 573-1121, Japan*
[2] *Institute of Dental Research, Osaka Dental University, 8-1, Kuzuhahanazonocho, Hirakata, Osaka 573-1121, Japan*
[3] *Department of Biomedical Engineering, National Cerebral and Cardiovascular Center Research Institute, Suita, Osaka 565-8565, Japan*
Corresponding author, Yoshitomo HONDA; E-mail: honda-y@cc.osaka-dent.ac.jp

Heparin binds to and modulates various growth factors, potentially augmenting the bone-forming capability of biomaterials. Here, α-tricalcium phosphate (α-TCP) granules were modified with peptide containing the marine mussel-derived adhesive sequence, which reacts with α-TCP surface, and cationic sequence, which binds to heparin (α-Ph). α-Ph retained the α-TCP phase and intergranule spaces after the surface modification. The existence of heparin on α-Ph granules was confirmed using X-ray photoelectron spectroscopy. Granules of α-TCP and α-Ph were implanted into critical-size defects in rat calvaria for 4 weeks. Micro-computed tomography, histological evaluation, and Alcian blue staining revealed that α-Ph induced superior bone formation compared with α-TCP. Newly formed bone on α-Ph was preferentially in contact with the Alcian blue-stained surfaces of granules. These results suggested that heparinization enhanced the early osteogenic capacity of α-TCP, possibly by modulating the secretion of Alcian blue-stained extracellular matrixes.

Keywords: Heparin, Calcium phosphate, α-Tricalcium phosphate, Critical size defects, Surface modification

INTRODUCTION

The reconstruction of bone defects caused by injury, infection, and tumor growth is crucial in maxillofacial surgery, dentistry, and orthopedics. Recently, numerous studies have reported that biodegradable calcium phosphates, such as alpha tricalcium phosphate (α-TCP, α-$Ca_3(PO4)_2$), β-TCP, carbonate apatite, and octacalcium phosphate (OCP), can be substituted by the bone tissue over time through the bone remodeling processes[1-4]. Some biodegradable calcium phosphates have been extensively investigated and applied for treating the site of bone defects to stabilize dental implants[5,6].

α-TCP is generally prepared by heat treatment of β-TCP and amorphous precursors[2]. Although these two compounds have similar chemical constitutions, α-TCP has greater degradability than β-TCP under physiological pH conditions[3]. The ceramics have been reported to dissolve in rabbit[1] and rat[7] cranial defects. α-TCP is the precursor of hydroxyapatite (HA). X-ray diffraction (XRD) analysis confirmed that the crystal phase of α-TCP spontaneously and irreversibly converts to the thermodynamically stable apatite phase in simulated body fluid *in vitro*[8]. As with other precursors, such as OCP, this conversion process accompanies the modulation of calcium ions and phosphate ions from the surrounding solution[4,8]; these two ions are known to induce the osteoblastogenesis *in vitro*[9,10]. Based on this background, our group and other researchers have recognized α-TCP and its composite with organic substances as prospective bone substitute materials and intensively investigated these materials in bone regenerative therapy[1,6,7,11,12]. However, there is still room for improvement of the bone-forming capacity of this material, compared with that induced by autogenous bone grafts, the gold standard treatment for bone defects.

Heparin, belonging to a class of glycosaminoglycans (GAGs), is known to have anticoagulant and antithrombotic effects and has therefore been experimentally applied in clinical practices since the 1920s[13]. Sulfated heparin interacts with basic molecules and proteins, such as cytokines, morphogens, and growth factors, due to its anionic charge[13]. This interaction promotes wound healing by protecting growth factors from nonenzymatic glycosylation and antagonists[14,15] and by working as an endogenous receptor, thereby leading to induction of biological modulation, such as cell proliferation, differentiation, and angiogenesis[16]. Numerous researchers have reported that heparin exhibits a variety of pharmacological effects, such as anti-inflammatory[17] and antimetastatic effects[13]. Consequently, immobilization of heparin on the material surface may be a promising method to regulate biological reactions of original material[18,19] and to provide a controlled release system[20]. In fact, we have previously reported that the immobilization of heparin to polyethylene specimens facilitates angiogenesis when the complex is implanted in the subcutaneous pocket of rats in comparison with that without heparinization[21]. Nevertheless, there are no studies evaluating the effects of heparinization on the α-TCP surface on bone-forming capacity.

Accordingly, the goal of this study was to

Color figures can be viewed in the online issue, which is available at J-STAGE.

Received Aug 24, 2017: Accepted Oct 18, 2017
doi:10.4012/dmj.2017-305 JOI JST.JSTAGE/dmj/2017-305

investigate whether surface treatment of α-TCP by the immobilization of heparin modulates its early osteogenic capability in critical sized defects in rat calvaria. To enhance the adsorption of heparin onto α-TCP granules, we utilized surface modification peptide (SMP), which bridges calcium phosphate and heparin. The peptides were composed of two different sequences: (1) the marine mussel-derived adhesive sequence, which reacts with various material surfaces, including α-TCP; and (2) the penta-lysine sequence, which shows electrostatic binding to heparin. Hereafter, α-TCP modified with the heparin-SMP complex is designated as α-Ph (α-TCP-peptide-heparin).

MATERIALS AND METHODS

Preparation of heparinized α-TCP granules

Figure 1A shows the schematic image of α-Ph composed of heparin, SMP, and α-TCP granules. Porous α-TCP granules (approximately 500–600 μm in diameter) were kindly provided by Taihei Chemical Industrial (Osaka, Japan). SMP was purchased from SCRUM (Tokyo, Japan). The sequence of SMP was as follows: (Lys)5-(Gly)3-Ala-Lys-Pro-Ser-Tyr-(Hyp)2-Thr-DOPA-Lys (DOPA; L-3,4-dihydroxyphenylalanine). Distilled water and heparin solution were supplied by Mochida Pharmaceutical (Tokyo, Japan). α-TCP porous granules sterilized by dry heat were placed in a 10 mg/mL aqueous solution of peptide for 24 h at 50°C. After washing with distilled water, the peptide-immobilized α-TCP porous granules were naturally dried onto a clean bench. Subsequently, the peptide-immobilized α-TCP porous granules were allowed to react in heparin solution (10,000 U/10 mL) for 8 h at room temperature. After washing with distilled water, α-Ph was naturally dried onto the clean bench.

Characterization of heparinized and nonheparinized α-TCP granules

A field emission-scanning electron microscope (FE-SEM: S-4800, Hitachi High-Technologies, Tokyo, Japan) was utilized to confirm the sizes and surface conditions of α-TCP and α-Ph granules. Pore distribution and interparticle sizes of both granules before implantation were evaluated by the mercury intrusion technique using an Auto Pore IV 9510 (Micro-metrics, Norcross, GA, USA). The crystal phase of α-TCP was identified using an XRD system (XRD-6100, Shimadzu, Kyoto, Japan) and database from the International Center for Diffraction Data (α-TCP: 9-0348). X-ray photoelectron spectroscopy (XPS; PHI X-tool, ULVAC-PHI, Kanagawa, Japan) was used to confirm the attachment of heparin and SMP on the surface of the α-TCP.

Implantation of heparinized and nonheparinized α-TCP granules into critical size bone defects in the rat calvaria

All animal experiments conformed to the Guiding Principles for the Use of Laboratory Animals and were approved by the Animal Experiment Committee

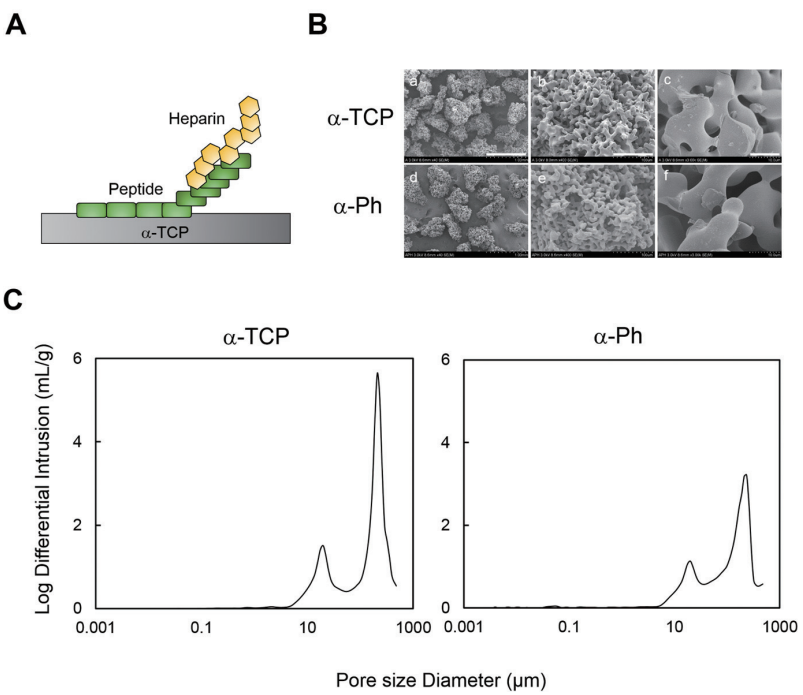

Fig. 1 Schematic images of α-Ph (A), scanning electron microscopic images (B), and intergranule sizes (C).
Bars in (B): 1 mm for a, d; 100 μm for b, e; 10 μm for c, f.

of Osaka Dental University (approval number: 16-03012). Sprague Dawley rats (male, 8 weeks old) were anesthetized pre-operatively with pentobarbital and isoflurane inhalation. An L-shaped incision was made in the skin and periosteum to avoid the defect area and prevent alteration of the bone-forming process. Critical size defects (9 mm in diameter) were created in each rat in the center of the calvaria using a trephine bar (Dentech, Tokyo, Japan)[22]. Sterile saline was used for irrigation during the procedure to prevent thermal damage of bones. The defects were filled with α-TCP or α-Ph granules, and the periosteum and skin were then overlaid and firmly sutured to stabilize the granules. Five rats were used for both groups. At 4 weeks after implantation, rats were sacrificed, and the treated calvariae were harvested to verify the bone-forming abilities of α-TCP and α-Ph as described below.

Micro-computed tomography (micro-CT)

Harvested calvariae were fixed with 4% paraformaldehyde in phosphate-buffered saline (Nacalai Tesque, Kyoto, Japan) and evaluated using micro-CT (SMX-130-CT, Shimadzu). Calvariae were exposed to 76 μA of 57 kV radiation. Images were saved as 512×512 pixels. Vertical and lateral views of calvariae were reconstructed using TRI/3D bone software (Ratoc, Tokyo, Japan). Bone mineral density (BMD) representing calcified bone tissue was assayed using cylindrical phantoms containing HA (HA content: 200–800 mg/cm^3). The radiopaque volume per total tissue volume (RV/TV) and mineral content per TV (MC/TV) were calculated to assess the mineralized tissue volume and weight in defects. Using the lateral BMD images, we further evaluated the maximum thickness of bone tissue with granules in the defects.

Histological and histomorphometric analysis of bone defects

Fixed calvariae were decalcified, dehydrated, and embedded in paraffin. The specimens were sectioned at 5-μm thickness and stained with hematoxylin-eosin (H-E) stain. Histomorphometric analysis of bone formation in the defects was carried out using Photoshop Elements (Adobe Systems, San Jose, CA, USA) and Image J (version 1.4.3.67, NIH, Rockville, MD, USA), as reported previously[23]. Briefly, H-E-stained sections covering the whole defect were used to calculate the extent of new bone formation. The area of tissue showing a color similar to that of the untreated calvaria was estimated as the area of newly formed bone (NB area), whereas the whole area created by the trephination was considered the treated area (TA). The percentage of newly formed bone was calculated as NB/TA×100. Alcian blue staining is known to stain heparin and other GAGs[24]. The staining was used to elucidate the mechanism of bone formation on α-Ph. Briefly, sections were deparaffinized and hydrated with distilled water, followed by treatment with 3% acetic acid solution and staining with Alcian blue solution (pH=2.5). The solution stained sulfated and nonsulfated acidic carbohydrates. The sections were washed with 3% acetic acid solution and distilled water. Kernechtrot staining was used for counter staining. Nine granules in three specimens were randomly measured to evaluate the blue-stained areas of both granules. Twelve granules in three specimens were measured to assess the length of the blue-stained surface, bone-granule contact surface, and no bone-granule contact surface using Image J.

Statistical analysis

Results are presented as means±standard deviations (SDs). Student's *t* tests were used to compare the two groups. Differences with *p* values of less than 0.01 and 0.05 were considered significant.

RESULTS

SEM images of α-TCP and α-Ph are shown in Fig. 1B. Both granules had a highly porous structure with smooth surfaces. Despite modification of the α-TCP surface by heparin-SMP, α-Ph showed negligible differences in granule size and surface conditions. Intergranule sizes (median diameter) before implantation were 209 μm for α-TCP and 174 μm for α-Ph (Fig. 1C). The XRD pattern obtained in α-Ph possessed the specific peak of α-TCP (indicated by triangles), whereas there was no peak for apatite (2θ=10.8; Fig. 2A). Sulfate (S2p) and nitrogen (N1s) peaks representing the existence of heparin and SMP were detected in the XPS peak of α-Ph (Fig. 2B). These results indicated that α-Ph was successfully overlaid by SMP and heparin but that the crystal structure of α-TCP was retained.

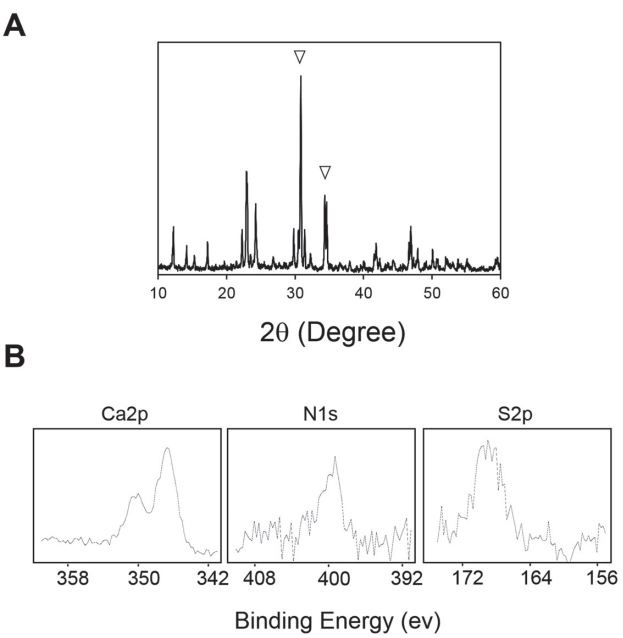

Fig. 2 XRD pattern (A) and X-ray photoelectron spectroscopy peaks (B) of α-Ph.
White triangles: specific peak of α-TCP.

Figures 3A and B show the micro-CT and BMD images of α-TCP and α-Ph groups captured from vertical and lateral sides, respectively. The radiopaque area of the α-Ph group in the defect was larger than that of the α-TCP group. Consistent with these images, the RV/TV and MC/TV of α-Ph were greater than those of α-TCP (Fig. 3C). Conversely, there were no significant differences in the maximum thickness of mineralized tissue in defects implanted with α-TCP and α-Ph. H-E staining revealed that both α-TCP and α-Ph were partially surrounded by the newly formed bone (Fig. 4A). Numerous multinucleated cells covered the α-TCP granules (Fig. 4A; high-magnification view of α-TCP, black arrows). In histomorphometric analysis, the NB area of α-Ph in defects was larger than that of α-TCP (Fig. 4B). These results indicated that surface modification by heparin-SMP significantly augmented early bone formation of α-TCP.

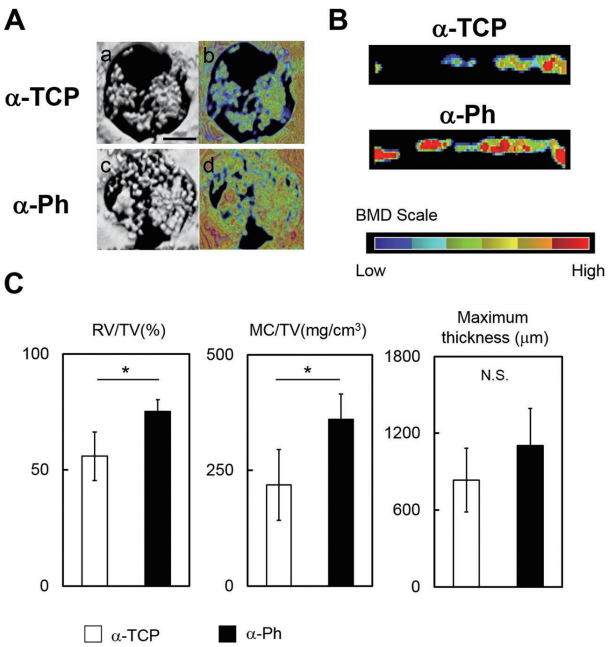

Fig. 3 Micro-computed tomography and BMD images of defects treated with α-TCP or α-Ph at 4 weeks after implantation (A, B).
(A) Vertical view; (B) lateral view. (a, b) α-TCP; (c, d) α-Ph. BMD scale in (B): degree of mineralization. Bar: 3 mm. (C) A quantitative image analysis. RV: radiopaque volume; TV: total volume; MC: mineral content. Maximum thickness: maximum thickness of lateral BMD images in (B). *p<0.05, means and SDs (n=5, Student's t test). N.S.: not significant.

Figures 5 and 6 show images of Alcian blue-stained sections of the bone defects treated with α-TCP and α-Ph at 4 weeks after implantation and corresponding quantitative data. Strong blue staining partially existed inside of the newly formed bone (Figs. 5Aa and Ac, white arrows), indicating that both samples were stained. However, blue stained area in α-Ph granules was greater than that in the α-TCP granules (Fig. 6A). Notably, α-Ph surfaces were strongly stained with Alcian blue (Figs. 5Ab and Ad, black arrows). The blue staining preferentially existed at the interface between the α-Ph granule surface and contacted bone (Fig. 5B). The percentage of bone contacting the blue-stained surface was about 73. The percentage of blue staining of the total bone-contacting surface was about 90 (Figs. 6B and C). These results suggested that new bone preferentially formed on the blue-stained surface of α-Ph granules.

DISCUSSION

In the present study, we designed heparinized α-TCP (α-Ph) using SMP containing the cationic sequence and the marine mussel adhesive sequence. α-Ph showed

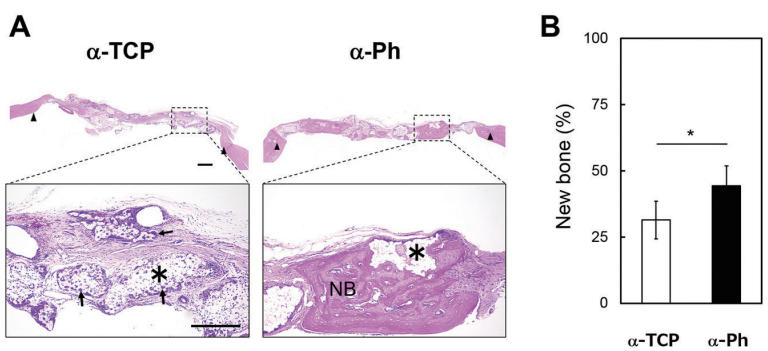

Fig. 4 Histological and histomorphometric analyses of defects treated with α-TCP or α-Ph at 4 weeks after implantation.
(A) H-E-stained sections at low- and high-magnification. Bars: 600 μm for low magnification and 300 μm for high magnification. Asterisks: implanted granules. Arrows: multinucleated giant cells. Gap between black triangles: created bone defect. NB: newly formed bone. (B) Quantitative analysis of new bone percentage in the defects. *p<0.05, means and SDs (n=5, Student's t test).

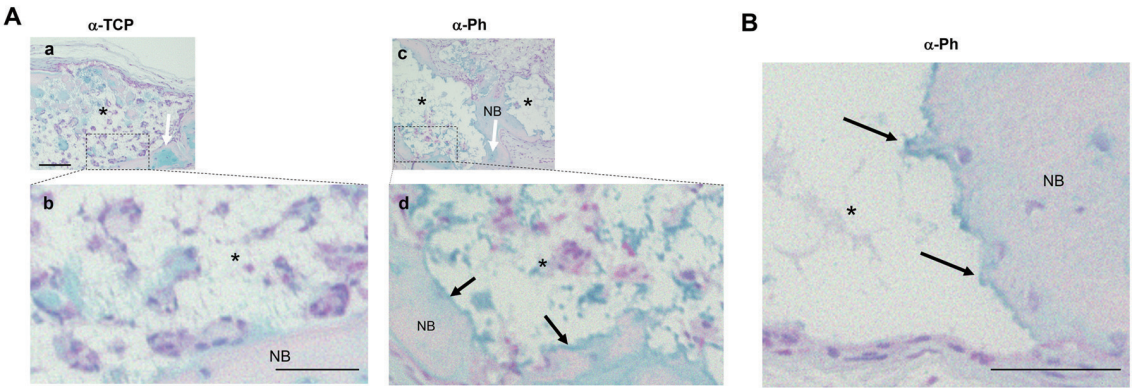

Fig. 5 Alcian blue-stained sections of defects treated with α-TCP or α-Ph at 4 weeks after implantation. (Aa and Ac) Low-magnification images. (Ab and Ad) High-magnification images. Bars: 100 μm for Aa and Ac; 50 μm for Ab and Ad. White arrows: blue staining in the bone. Black arrows: surface stained with Alcian blue. NB: newly formed bone. Asterisks: implanted granules. (B) Representative image of blue staining at the interface of the new bone area and α-Ph. Bar: 25 μm.

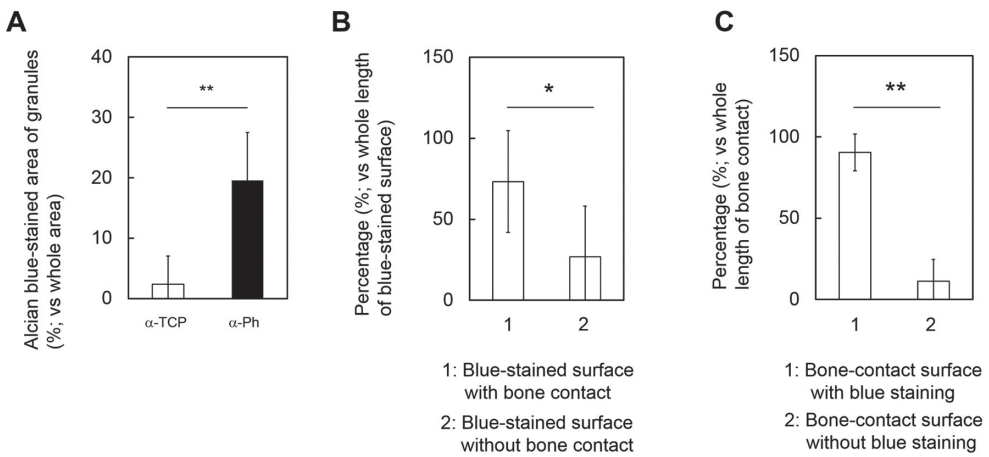

Fig. 6 Quantitative analysis of Alcian blue-stained sections on α-TCP and α-Ph. (A) Percentage of the area stained by Alcian blue on α-TCP and α-Ph granules. $^{**}p<0.01$, means and SDs (n=9, randomly selected from different three specimens; Student's t test). (B) Percentage of the blue-stained surface with/without bone granule contact. (C) Percentage of the bone granule contact surface with/without blue staining. $^{*}p<0.05$, $^{**}p<0.01$, means and SDs (n=12, randomly selected from different three specimens; Student's t test).

greater bone formation than α-TCP. Quantitative analysis using Alcian blue staining provided evidence that new bone formation preferably occurred on the blue-stained surface.

Steric and topographic conditions attributed to pore size, porosity, and intergranule space are known to be associated with the bone-forming capacity of calcium phosphates[25,26]. Numerous studies have reported that α-TCP is converted into octacalcium[27] and Ca-deficient apatite *in vitro*, depending on the working conditions[8]. SEM images in previous studies have revealed that these transformations change the surface structure and form of α-TCP[8,27], possibly altering the pore size and intergranule spaces. Additionally, the crystal phase should severely alter the bone-forming capacity of calcium phosphates. In the present study, surface modification in water may alter the steric and topographic conditions of α-Ph from α-TCP. However, there were negligible difference in pore size and intergranule space after modification by heparin and SMP (Figs. 1B and C); α-Ph retained the crystal phase of α-TCP (Fig. 2A). Significant differences were observed in early bone formation induced by α-TCP and α-Ph (Figs. 3 and 4). These results supported that the superiority of the bone-forming capacity of α-Ph compared with that of α-TCP was likely due to the effects of surface modification with heparin.

Unfortunately, we have not yet determined the

mechanisms underlying the enhancement of the bone-forming capacity of α-Ph. Although previous various studies have investigated the effects of heparin on osteoblast differentiation, its effects are still controversial. Some studies have reported that single use of heparin inhibits alkaline phosphatase secretion and mineralization[28,29], while other studies have shown that the polysaccharide increases mineralization[30,31]. Hausser and Brenner reported that the effects are mainly dependent on the concentration of the molecule[30]. Based on these studies, surface modification of α-TCP by heparin-SMP itself may directly enhance the bone-forming capacity of α-TCP at an adequate dose of heparin.

Heparin can bind to various growth factors, such as basic fibroblastic growth factor (bFGF), transforming growth factor, and bone morphogenic protein[13]. This polysaccharide modulates or conserves the bioactivity of the molecules[15]. We have previously reported that porous polyethylene modified by heparin-peptide could support bFGF immobilization and could be used as a controlled-release carrier for this growth factor[21]. The heparin-SMP immobilized polymer with bFGF could accelerate tissue integration in murine subcutaneous pockets. Additionally, implantation of α-Ph with bFGF markedly enhances bone formation in a canine mandibular bone defect model[32]. Furthermore, endogenous growth factors are abundantly secreted *in vivo* and are involved in various biological reactions. These results suggest that heparin in α-Ph may accumulate endogenous growth factors and other osteogenic molecules, resulting in efficient promotion of early bone formation. Although this hypothesis would be attractive in terms of cost and complications upon intervention using exogenous growth factors, we have no critical evidence that growth factors were strongly accumulated at the surface of α-Ph. Thus, further experiments are needed to prove this hypothesis.

Our most striking finding was that new bone formation preferentially occurred on the surface of α-Ph with blue staining (Figs. 5 and 6). Initially, we speculated that blue staining at the surface of α-Ph was due to the heparin-SMP[24,33]. However, we did not observe such a blue staining on the surface of α-Ph before implantation, possibly due to its low content (data not shown). Additionally, there was poor blue staining at the interface between new bone and α-TCP (Fig. 5A). These results indicated that the surface of α-Ph induced blue-stained substances to a greater extent than α-TCP after operation.

Notably, Alcian blue staining can target not only heparin but also other GAGs, such as chondroitin sulfate, dermatan sulfate, and heparan sulfate[33,34]. Chondroitin sulfate E and bone morphogenic protein 4 have the potential to induce cell growth, alkaline phosphatase activity, and mineralization of osteoblastic cells *in vitro*[31]. Heparan sulfate can be a coreceptor of bone morphogenic protein[35], and that growth factor is a strong stimulant of osteogenesis. GAGs modulate bone morphogenic protein 4 signaling[36]. Bone marrow-derived heparan sulfate augments the bone-forming capacity of bone morphogenic protein 2[37]. Given these previous studies and our findings of the difference in Alcian blue staining on the surface of α-TCP and α-Ph (Figs. 5 and 6), surface modification of α-TCP by heparin-SMP may modulate the secretion of extracellular matrix components, such as GAGs, from the cells, thereby accelerating bone formation.

CONCLUSION

In the present study, we demonstrated that surface modification of α-TCP with heparin-SMP significantly enhanced early bone formation in critical size defects in rat calvaria within 4 weeks after implantation. Alcian blue staining at 4 weeks after implantation revealed that new bone formed on α-Ph preferentially existed on surfaces stained with Alcian blue. Although we could not identify the blue-stained substances, our results may indicate that surface modification by heparin-SMP on α-TCP modulated the extracellular secretion of substances such as GAGs from the cells surrounding the granules. The secreted extracellular matrix may effectively accelerate early bone formation induced by α-Ph. These results provide insights into the effects of surface modifications of biomaterials, such as calcium phosphate, in bone regeneration therapy. However, further detailed experiments, such as long-term tracking of bone formation and/or as using other doses of heparin-SMP, are essential for fabrication of a safe and reliable material for clinical use.

ACKNOWLEDGMENTS

The study was partially supported by the JSPS KAKENHI Grant Number 25463062 and 16K11667 and by the Japan Agency for Medical Research and Development (No. 15ek0109138h001). We thank Akihisa OTAKA (Department of Biomedical Engineering, National Cerebral and Cardiovascular Center Research Institute) for technical support to prepare heparin-SMP. We also thank Yoshiya HASHIMOTO (Department of Biomaterials, Osaka Dental University) and Naoya UEMURA (Department of Oral Implantology, Osaka Dental University) for the advice of the animal experiments, and Hideaki HORI (Institute of Dental Research, Osaka Dental University) for the technical advice for the SEM observation.

REFERENCES

1) Yamada M, Shiota M, Yamashita Y, Kasugai S. Histological and histomorphometrical comparative study of the degradation and osteoconductive characteristics of alpha- and beta-tricalcium phosphate in block grafts. J Biomed Mater Res B Appl Biomater 2007; 82: 139-148.
2) Carrodeguas RG, De Aza S. alpha-Tricalcium phosphate: synthesis, properties and biomedical applications. Acta Biomater 2011; 7: 3536-3546.
3) Ishikawa K. Bone substitute fabrication based on dissolution-precipitation reactions. Materials 2010; 3: 1138-1155.

4) Suzuki O. Octacalcium phosphate (OCP)-based bone substitute materials. Jpn Dent Sci Rev 2013; 49: 58-71.
5) Saska S, Mendes L, Gaspar A, Capote T. In: Turkyilmaz I, editor. Current concepts in dental implantology: InTech; 2015. p. 26-58.
6) Hirose M, Uemura N, Hashimoto Y, Toda I, Baba S. Bone augmentation of canine frontal sinuses using a porous α-tricalcium phosphate for implant treatment. J Oral Sci Rehabil 2017; 3: 44-51.
7) Kihara H, Shiota M, Yamashita Y, Kasugai S. Biodegradation process of alpha-TCP particles and new bone formation in a rabbit cranial defect model. J Biomed Mater Res B Appl Biomater 2006; 79: 284-291.
8) Uchino T, Yamaguchi K, Suzuki I, Kamitakahara M, Otsuka M, Ohtsuki C. Hydroxyapatite formation on porous ceramics of alpha-tricalcium phosphate in a simulated body fluid. J Mater Sci Mater Med 2010; 21: 1921-1926.
9) Dvorak MM, Siddiqua A, Ward DT, Carter DH, Dallas SL, Nemeth EF, Riccardi D. Physiological changes in extracellular calcium concentration directly control osteoblast function in the absence of calciotropic hormones. Proc Natl Acad Sci U S A 2004; 101: 5140-5145.
10) Beck G. Inorganic phosphate regulates multiple genes during osteoblast differentiation, including Nrf2. Exp Cell Res 2003; 288: 288-300.
11) Tokuda T, Honda Y, Hashimoto Y, Matsumoto N. Comparison of the bone forming ability of different sized-alpha tricalcium phosphate granules using a critical size defect model of the mouse calvaria. Nano Biomed 2015; 7: 63-71.
12) Li P, Hashimoto Y, Honda Y, Arima Y, Matsumoto N. The effect of interferon-gamma and zoledronate treatment on alpha-tricalcium phosphate/collagen sponge-mediated bone-tissue engineering. Int J Mol Sci 2015; 16: 25678-25690.
13) Mulloy B, Hogwood J, Gray E, Lever R, Page CP. Pharmacology of heparin and related drugs. Pharmacol Rev 2016; 68: 76-141.
14) Nissen NN, Shankar R, Gamelli RL, Singh A, DiPietro LA. Heparin and heparan sulphate protect basic fibroblast growth factor from non-enzymic glycosylation. Biochem J 1999; 338: 637-642.
15) Honda Y, Ding X, Mussano F, Wiberg A, Ho CM, Nishimura I. Guiding the osteogenic fate of mouse and human mesenchymal stem cells through feedback system control. Sci Rep 2013; 3: 3420.
16) Olczyk P, Mencner L, Komosinska-Vassev K. Diverse roles of heparan sulfate and heparin in wound repair. Biomed Res Int 2015; 2015: 549417.
17) Mousavi S, Moradi M, Khorshidahmad T, Motamedi M. Anti-inflammatory effects of heparin and its derivatives: a systematic review. Adv Pharmacol Sci 2015; 2015: 507151.
18) Murugesan S, Xie J, Linhardt RJ. Immobilization of heparin: approaches and applications. Curr Top Med Chem 2008; 8: 80-100.
19) Wu Q, Li Y, Wang Y, Li L, Jiang X, Tang J, Yang H, Zhang J, Bao J, Bu H. The effect of heparinized decellularized scaffolds on angiogenic capability. J Biomed Mater Res A 2016; 104: 3021-3030.
20) Knaack S, Lode A, Hoyer B, Rosen-Wolff A, Gabrielyan A, Roeder I, Gelinsky M. Heparin modification of a biomimetic bone matrix for controlled release of VEGF. J Biomed Mater Res A 2014; 102: 3500-3511.
21) Kakinoki S, Sakai Y, Fujisato T, Yamaoka T. Accelerated tissue integration into porous materials by immobilizing basic fibroblast growth factor using a biologically safe three-step reaction. J Biomed Mater Res A 2015; 103: 3790-3797.
22) Vajgel A, Mardas N, Farias BC, Petrie A, Cimoes R, Donos N. A systematic review on the critical size defect model. Clin Oral Implants Res 2014; 25: 879-893.
23) Honda Y, Anada T, Kamakura S, Morimoto S, Kuriyagawa T, Suzuki O. The effect of microstructure of octacalcium phosphate on the bone regenerative property. Tissue Eng Part A 2009; 15: 1965-1973.
24) Somasundaram S, Vijayabaskar P. Histological and analytical evaluation of glycosaminoglycan from the clam katelysia opima. Trends Med Res 2007; 2: 165-175.
25) Galois L, Mainard D. Bone ingrowth into two porous ceramics with different pore sizes: an experimental study. Acta Orthop Belg 2004; 70: 598-603.
26) Hannink G, Arts JJ. Bioresorbability, porosity and mechanical strength of bone substitutes: what is optimal for bone regeneration? Injury 2011; 42 Suppl 2: S22-25.
27) Bigi A, Boanini E, Botter R, Panzavolta S, Rubini K. Alpha-tricalcium phosphate hydrolysis to octacalcium phosphate: effect of sodium polyacrylate. Biomaterials 2002; 23: 1849-1854.
28) Bhandari M, Hirsh J, Weitz J, Young E, Venner T, Shaughnessy S. The effects of standard and low molecular weight heparin on bone nodule formation in vitro. Thromb Haemost 1998; 80: 413-417.
29) Kanzaki S, Takahashi T, Kanno T, Ariyoshi W, Shinmyouzu K, Tujisawa T, Nishihara T. Heparin inhibits BMP-2 osteogenic bioactivity by binding to both BMP-2 and BMP receptor. J Cell Physiol 2008; 216: 844-850.
30) Hausser HJ, Brenner RE. Low doses and high doses of heparin have different effects on osteoblast-like Saos-2 cells in vitro. J Cell Biochem 2004; 91: 1062-1073.
31) Miyazaki T, Miyauchi S, Tawada A, Anada T, Matsuzaka S, Suzuki O. Oversulfated chondroitin sulfate-E binds to BMP-4 and enhances osteoblast differentiation. J Cell Physiol 2008; 217: 769-777.
32) Kobayashi N, Hashimoto Y, Otaka A, Yamaoka T, Morita S. Porous alpha-tricalcium phosphate with immobilized basic fibroblast growth factor enhances bone regeneration in a canine mandibular bone defect model. Materials 2016; 9: 853.
33) Noborn F, O'Callaghan P, Hermansson E, Zhang X, Ancsin JB, Damas AM, Dacklin I, Presto J, Johansson J, Saraiva MJ, Lundgren E, Kisilevsky R, Westermark P, Li JP. Heparan sulfate/heparin promotes transthyretin fibrillization through selective binding to a basic motif in the protein. Proc Natl Acad Sci U S A 2011; 108: 5584-5589.
34) Cowman M, Slahetka M, Hittner D, Kim J, Forino M, Gadelrab G. Polyacrylamide-gel electrophoresis and Alcian Blue staining of sulphated glycosaminoglycan oligosaccharides. Biochem J 1984; 221: 707-716.
35) Kuo WJ, Digman MA, Lander AD. Heparan sulfate acts as a bone morphogenetic protein coreceptor by facilitating ligand-induced receptor hetero-oligomerization. Mol Biol Cell 2010; 21: 4028-4041.
36) Khan SA, Nelson MS, Pan C, Gaffney PM, Gupta P. Endogenous heparan sulfate and heparin modulate bone morphogenetic protein-4 signaling and activity. Am J Physiol Cell Physiol 2008; 294: C1387-1397.
37) Bramono DS, Murali S, Rai B, Ling L, Poh WT, Lim ZX, Stein GS, Nurcombe V, van Wijnen AJ, Cool SM. Bone marrow-derived heparan sulfate potentiates the osteogenic activity of bone morphogenetic protein-2 (BMP-2). Bone 2012; 50: 954-964.